*Combustion, Explosion, and Shock Waves, Vol. 49, No. 3, pp. 325–334, 2013.*
*Original Russian Text © A.P. Ershov.*

# Regimes of Detonation of Solid Explosives with Nonclassical Fast Kinetics

**A. P. Ershov**[a]

UDC 662.215.1

Translated from *Fizika Goreniya i Vzryva*, Vol. 49, No. 3, pp. 77–87, May–June, 2013.
Original article submitted April 6, 2012.

**Abstract:** Detonation development in a system whose exothermal reaction kinetics depends on the rate of change of the specific volume is studied numerically. In the case of sudden compression, e.g., in a shock front, this kinetics leads to a finite degree of conversion. If the contribution of such fast processes is significant, detonation regimes that differ from the standard Zel'dovich–Neumann–Döring regime are obtained. The wave profiles qualitatively coincide with those obtained for some explosives by Utkin et al. The modeling confirms the importance of fast processes in the wave front.

*Keywords*: macrokinetics, high explosives, reaction zone structure, nonideal detonation, weak detonation.

**DOI:** 10.1134/S001050821303009X

## INTRODUCTION

It is known that detonation of condensed high explosives (HEs) occurs most often in the Zel'dovich–Neumann–Döring (ZND) regime. The majority of methods used to study reaction kinetics are based on this fact. In the simplest cases, the reaction time is estimated on the basis of the von Neumann peak duration. In more detailed approaches, the kinetics that ensures the most adequate description of experimentally observed profiles is sought. The most popular parameter measured in recent studies is the velocity history of the interface between the HE and the inert window.

Sometimes, however, the peaks expected in the ZND regime were not observed. Naturally, it is impossible to extract the kinetics based on the ZND model from the experiment in such cases. In some experiments, reduced peaks of significantly lower amplitude were obtained. In such cases, additional measures should be taken to reconcile the kinetics with experimental data. In what follows, we refer to all such detonation regimes as nonclassical regimes, in contrast to the "pure" ZND case.

The chemical peak was not detected in [1, 2] at a high HE density. In principle, it is possible within the framework of the ZND model if the reaction is fast enough to keep the peak within the limits of experimental resolution (≈5 ns). The qualitative change in the wave structure with a smooth pressure increase was observed in [3]. Note that the chemical peak was obtained in [4] under conditions similar to [1, 3] ("agatized" HEs, i.e., HEs pressed to a high density with addition of acetone). Such discrepancies my indicate the important role of the HE preparation procedure, which determines, in particular, the charge structure. The most representative set of data including obviously nonclassical cases can be found in [5–14]. A large variety of HEs in a wide range of initial densities and particle sizes were studied. The velocity history of foil driven by the HE charge was measured when the wave went out to a transparent window (water or LiF). As heterogeneous porous materials were studied, the foil thickness had to be rather large (hundreds of micrometers), which allowed the velocity profile to be recorded during 150–200 ns. This approach made it possible to observe qualitative changes in the reaction zone structure depending on the initial density, with other test conditions being unchanged. The absence of any significant distortions of the signal in foil was convincingly demonstrated

[a]Lavrent'ev Institute of Hydrodynamics, Siberian Branch, Russian Academy of Sciences, Novosibirsk, 630090 Russia; ers@hydro.nsc.ru.

in [12–14]. In many cases, quantitative deviations from the ZND regime were observed, in particular, extremely small amplitudes of the von Neumann peaks. Moreover, qualitative differences were also observed, namely, the shape of the profiles with increasing particle velocity (and, hence, pressure) behind the shock wave.

Such obviously nonclassical profiles were obtained for RDX, HMX, TNETB, and ZOX at high densities beginning from 1.73, 1.84, 1.56, and 1.71 g/cm$^3$, respectively. RDX was pressed to densities of 1.50–1.74 g/cm$^3$ with addition of a small amount of acetone (within 1%). Higher densities (up to 1.776 g/cm$^3$) were reached by agatization with 10% of acetone, and a chemical peak was observed in such charges. Utkin et al. [7, 9] expected the chemical peak to vanish at higher densities of 1.78–1.79 g/cm$^3$, which were reached in [1, 3].

In the TNETB explosive, most intensively studied, researchers discovered an interval of initial densities (1.56–1.77 g/cm$^3$ or 84.8–96.2% of the crystalline density) in which a gradual increase in the interface velocity was observed instead of the chemical peak [11–14]. For some HEs, the initial particle size was demonstrated to play an important role. In fine-grained (5 $\mu$m) TNETB, the transition to the nonclassical regime occurred already at a density of about 1.3 g/cm$^3$. In RDX with the same particle size, the nonclassical regime occurred in a small vicinity of the density value of 1.3 g/cm$^3$ [10]. All these observations indicate an important role of the HE structure, which is determined by the initial particle size and by the charge preparation procedure rather than by the pressing density only. Though regimes without the chemical peak were initially associated with almost homogeneous agatized charges, a more detailed analysis shows that a heterogeneous structure is preferable for obtaining these regimes.

The results obtained in [5–14] were attributed by the authors to deviations from the classical ZND regime. The width of the compression region in the detonation wave front in heterogeneous HEs is of the order of the characteristic pore size; therefore, it is a macroscopic quantity. Within these limits, the HE can partially react. As a result, the von Neumann peaks can decrease or even disappear in the case of significant burnout in the front. Situations with a gradual growth of parameters instead of the chemical peak are treated as weak detonation regimes. The same processes that lead to the chemical reaction in the front also ensure dissipation. It is known that dissipative mechanisms can lead to reduction of the chemical peak and to formation of weak detonation waves [15]. A typical feature of weak detonation (wave velocity higher than the Chapman–Jouguet thermodynamic velocity) was observed in [11, 12].

Thus, the existence of nonclassical regimes seems to be validated. The next problem is to extract the kinetics from experimental data. Conventional approaches based on the ZND model are inapplicable in such situations. The allowance for the reaction in a narrow zone within the wave front [16] or for the jump in the degree of conversion behind the shock [17, 18] can improve the description of regimes with a reduced chemical peak, but are not suitable for situations with inverted profiles.

In [19, 20], we considered the kinetics that allows finite burnout in the wave front. These works are based on the development of Trofimov's idea [21–23] about the explicit allowance for the Lagrangian rate of change of the specific volume $\partial V/\partial t$ in the kinetic equation. Formally, this approach is similar to taking into account differential terms when viscous forces are introduced. It was demonstrated [20] that the kinetics with explicit involvement of the derivative can describe regimes where the von Neumann peak is weakly expressed. The structure of the steady wave was studied in detail. However, more exotic cases with an increase in parameters behind the wave front were not considered.

In this work, we solve an unsteady problem of detonation wave formation from an initial perturbation. Based on a model example, we demonstrate that differential kinetics used in [20] with appropriate allowance for dissipation can generate not only modified Chapman–Jouguet regimes, but also weak detonation. Thus, a detailed qualitative description of nonclassical detonation waves observed experimentally is provided.

## 1. FORMULATION OF THE PROBLEM

A one-dimensional flow with chemical reactions is described by the following system of equations:

$$\frac{\partial V}{\partial t} - V_0 \frac{\partial u}{\partial x} = 0, \quad \frac{\partial u}{\partial t} + V_0 \frac{\partial p}{\partial x} = 0. \tag{1}$$

Here $t$ is the time, $x$ is the Lagrangian coordinate, $u$ is the flow velocity, $V$ is the specific volume of the substance, $V_0$ is the initial specific volume (which is constant for a homogeneous sample), and $p$ is the pressure. The energy equation has the form

$$\frac{\partial E}{\partial t} + p \frac{\partial V}{\partial t} = 0. \tag{2}$$

In what follows, we need an equation of state of the form $E = E(p, V, \lambda)$, where the degree of conversion $\lambda$ describes the chemical reactions. We assume that $\lambda$ changes from zero in the initial state to unity in the final equilibrium state. As we want to consider the simplest example of the problem solution, we confine ourselves to the idealized expression

$$E = \frac{pV}{\gamma - 1} - \lambda Q, \tag{3}$$

where the ratio of specific heats $\gamma$ and the thermal effect $Q$ are constants.

The system is closed by a kinetic equation written in the form [20]

$$\frac{\partial \lambda}{\partial t} = \frac{1-\lambda}{\tau} - b\frac{1-\lambda}{V_0}\frac{\partial V}{\partial t}, \tag{4}$$

where $\tau$ is the characteristic reaction time. In Eq. (4), the contribution of nonclassical differential kinetics is controlled by the dimensionless coefficient $b$. The positive sign of $b$ corresponds to reaction acceleration during compression (in particular, final conversion after passing the shock front).

If the compression from $V_0$ to $V$ is fast as compared with the time $\tau$ and the algebraic term is neglected, Eq. (4) yields the value of $\lambda$:

$$\lambda = 1 - \exp(-b(1 - V/V_0)). \tag{5}$$

Physical processes responsible for the reaction (collapse of pores, formation of microcumulative jets, etc.) can be considered as collisions of substance microvolumes, leading to nucleation of reaction sites. If these collisions occur on the background of overall compression of the medium ($\partial V/\partial t < 0$), then rapprochement of the structural elements can appreciably accelerate the reaction, which is reflected by the differential term in Eq. (4). Note that a linear (in terms of $\partial V/\partial t$) equation similar to Eq. (4) and an analog of Eq. (5) are used in the well-known kinetics proposed by Morozov and Karpenko [18] to describe finite burnout in reaction sites formed on the shock front.

As we are interested in wave processes where the reaction is triggered under compression, we assume that Eq. (4) is valid if the pressure at a given Lagrangian point exceeds a specified threshold value $p_i$ on the background of the initial value $p_0$. Variations of $p_i$ in the interval $(1.01–1.1)p_0$ did not exert any significant effect on the results. The calculations reported below were performed at $p_i = 1.03p_0$. When the reaction was initiated, the degree of conversion in accordance with Eq. (5) was prescribed simultaneously at all new points.

The computational domain consists of two parts. The subdomain $0 < x < 50$ mm is occupied by the HE. The right end face of the charge contacts with the inert window material 12.5 mm thick. As a whole, these sizes are similar to those used in real experiments. The left ($x = 0$) and right ($x = 62.5$ mm) boundaries are rigid walls ($u = 0$). A zero velocity is set in the entire interval at $t = 0$. The pressure is $p_0$ everywhere except for a small segment adjacent to the left boundary (initiation region). In this small region, complete burnout in a constant volume is prescribed ($\lambda = 1$, with a corresponding value of pressure). It should be noted that kinetics (4) is independent of the thermodynamic parameters $(p, V)$, which eliminates possible complications of unsteady interaction of the reaction zone with the wave reflected from the window material.

As in [20], we use the following values of the constants: $V_0 = 1$ cm$^3$/g, $\gamma = 2.7$, and $Q = 4$ kJ/g. The initial pressure is $p_0 = 1$ GPa. With these values, the basic parameters of the wave are close to real parameters for condensed HEs: detonation velocity $D_\text{J} = 7.456$ km/s, Chapman–Jouguet pressure $p_\text{J} = 15.294$ GPa, and specific volume in the Jouguet state $V_\text{J} = 0.7429$ cm$^3$/g. The window material has the same initial density and the same equation of state, but it is assumed to be inert. The characteristic reaction time $\tau$ is taken to be 30 ns, which is also close to the results of real experiments.

The presence of the derivative in the right side of the kinetic equation (4) changes the dynamic properties of the reacting medium. In particular, the velocity of small short-wave perturbations is modified [20]: the usual thermodynamic velocity of sound $c = \sqrt{\gamma p V}$ for the chosen dependences (3) and (4) is replaced by

$$c_E = \sqrt{\gamma p V + \frac{(\gamma - 1)bQ(1-\lambda)V}{V_0}}. \tag{6}$$

It should be noted that not only the algebraic term in Eq. (4), but also the contribution of the derivative vanishes in the case of complete burnout ($\lambda = 1$). As a result, the reaction zone is matched with the accompanying Taylor wave. One has $c_E = c$ everywhere in this wave as well as at the end of the reaction zone. Therefore, the thermodynamic Chapman–Jouguet velocity is the same as that in the ZND model (at $b = 0$).

## 2. NUMERICAL MODEL

To solve the unsteady problem, we use the classical Richtmyer–Morton scheme [24]. In this scheme, the shocks are captured by using artificial viscosity introduced on compression waves. In Eqs. (1) and (2), the viscous stress $q$ is added to the thermodynamic pressure:

$$\frac{\partial u}{\partial t} + V_0\frac{\partial (p+q)}{\partial x} = 0, \ \frac{\partial E}{\partial t} + (p+q)\frac{\partial V}{\partial t} = 0. \tag{7}$$

In the flow regions where the substance is compressed ($\partial u/\partial x < 0$), we have

$$q = \frac{Ah^2}{V}\left(\frac{\partial u}{\partial x}\right)^2,$$

otherwise $q = 0$. Here $h$ is the computational cell size and $A$ is a dimensionless coefficient. As was demonstrated in [24], such a form of viscosity ensures "smear-

ing" of the compression wave front, which is independent of the wave amplitude. It is this property that is desirable for modeling waves in heterogeneous materials where the characteristic width of the wave front is determined by the charge structure. The viscosity coefficient $A$ is varied from 4 to 16, and no noticeable effect on the results is observed. As we expand the inviscid formulation of [20] in this work, it is of interest to study low-viscosity flows, and the major part of calculations are performed with $A = 8$. In this case, the shock front is "smeared" approximately over four computational cells. The time step is determined from the Courant condition, which includes the true velocity of small perturbations $c_E$. As strong shock waves appear in the calculations, the Courant number is set equal to 0.3 to ensure stability of strong shocks.

For our problem, the use of quadratic viscosity has a more profound meaning than it is usually assumed. In computational fluid dynamics, this viscosity is regarded as artificial viscosity, and it usually exceeds real viscosity (it "smears" discontinuities much more significantly than real dissipation mechanisms do). Conversely, for heterogeneous porous substances, it is not a mere tool for organization of shock-capturing computations, but an actual characteristic of real processes. Dissipation in the compression wave front in a porous medium is related to the same collisions of microvolumes that lead to a fast reaction. Certainly, the actual reproduction of the shock wave structure in a real medium cannot be expected. Qualitatively, however, artificial viscosity "works" in the correct direction, and there are as many reasons to include it into the model to modify the kinetics as in Eq. (4). In the main series of calculations, the cell size was 1/160 mm, so the shock wave thickness was approximately 25 $\mu$m. During the characteristic reaction time $\tau$, the wave moved approximately over 35 cells.

It was demonstrated in the classical studies of the shock wave structure in gases [25, 26] that the molecular mechanisms of dissipation allow the shock wave structure to be resolved. The characteristic width of a weak wave is inversely proportional to its amplitude. For strong waves, the shock wave width is known to be of the order of the mean free path, and standard linear expressions for viscous stresses are no longer applicable. An analog of the mean free path in porous substances is the characteristic pore size. For wave amplitudes of interest, this size determines the width of the transitional zone from the initial to compressed state. Therefore, the use of quadratic viscosity of the form (7) is not only convenient, but also reflects the real situation.

Owing to the use of the shock-capturing algorithm, the process becomes evolutionary. Wave development

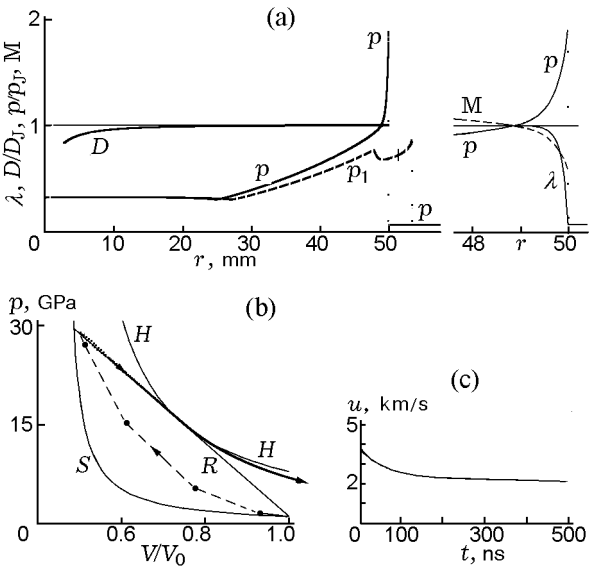


**Fig. 1.** Calculations based on the classical kinetics ($b = 0$): (a) distributions of parameters; (b) phase diagram; (c) record of interface velocity (the time is counted from the instant when the wave reaches the interface).

from the initial perturbation occurs naturally. It is shown below that both "normal" and weak detonation regimes are obtained in computations (which can be hardly expected from shock-fitting techniques). It should be noted that the algorithm proposed in [24] is not monotonic, and there are small fluctuations on the wave front. For our simple kinetics, which does not involve activation-type dependences, however, this drawback is not important.

## 3. CALCULATION RESULTS

First, it is natural to consider the case with $b = 0$, where the contribution of nonclassical differential kinetics is absent. Figure 1a (left) shows the pressure profile $p$ (hereinafter, the profiles are plotted as functions of the Eulerian coordinate $r$) at the time when the wave front reaches the interface between the charge and the window material and also the wave velocity $D$ as a function of the wave front coordinate. On the right graph, the profiles of pressure, flow Mach number (M) in the wave-front-fitted coordinate system, and degree of conversion $\lambda$ in the vicinity of the front are shown in more detail. It is seen that a detonation wave is formed, which has a clearly expressed chemical peak and the Chapman–Jouguet point (the value M = 1 is reached at $p = p_J$), followed by a self-similar Taylor wave and by a region with constant parameters. The wave velocity rapidly

reaches the ideal value $D_J$ (the calculated wave velocity is 7.471 km/s, which differs from $D_J$ by 0.2%).

Figure 1b shows the $p$–$V$ diagram of state in the wave at the same time instant. The phase trajectory starts from the point $(p_0, V_0)$, where it touches the shock adiabat $S$. After that, the point moves upward, staying between $S$ and the Rayleigh–Michelson line $R$, as it could be expected for the region of significant dissipation. This part of the trajectory is denoted by the dashed line connecting the calculation points. The trajectory approaches (but does not reach) the point of the upper intersection of $S$ and $R$ because of a partial reaction in the wave front. In the case considered, the reason for the moderate degree of conversion in the wave front is a finite width of the front determined by dissipation rather than the differential mechanism (because it is "turned off"). In the course of burning, the trajectory follows the line $R$ up to the point where it touches the Hugoniot adiabat $H$, and then goes below $H$ along the Poisson adiabat from the Chapman–Jouguet state. A weak scatter of points near the pressure maximum, which is caused by nonmonotonicity of the calculation scheme, is almost invisible at the scale of this figure.

The pressure distribution at 0.6 $\mu$s after the wave contact with the interface is shown in Fig. 1a by the dashed curve $p_1$. The shock wave passes to the inert substance, and the expansion wave propagates into the reacting medium. The vertical line on the graph shows the interface position at this instant. Figure 1c shows the calculated record of the interface velocity, which simulates the result of the VISAR test. In this record, one can see two qualitatively different segments: the initial segment with an approximately exponential decrease in velocity in accordance with kinetics (4) at $b = 0$ and the subsequent linear segment representing the Taylor wave. Estimating the reaction time by means of fitting the function $u(t) = F + Gt + H\exp(-t/T)$, we obtain $T = 67.3$ ns, i.e., this estimate overstates the true reaction time $\tau$ approximately by a factor of 2.

To find the reasons for this difference, we performed a special processing of numerical data. We constructed the profiles of $\lambda$ and $p$ as functions of the Lagrangian coordinate $x$ (measured from the front) at the instant when the wave reaches the interface. Like the dependences $u(t)$ discussed above, these profiles were approximated by the function $p(x) = p_1\exp(-x/p_2) + p_3 + p_4x$ or $\lambda(x) = L_0 - L_1\exp(-x/L_2)$. The first four points corresponding to the "smeared" shock wave were rejected. An almost perfect coincidence of the calculated points and the approximating function was observed. After that, we found the characteristic time of changing of each quantity from the relations $L_2 = D\tau_\lambda$ and $p_2 = D\tau_p$, which are valid because the wave reaches a steady state. The use of the Lagrangian coordinate allowed us to track the processes in a particle, excluding deformation distortions.

For the degree of conversion, the characteristic time $\tau_\lambda$ was accurately reproduced (after this processing, we obtained 29.993 ns), but the time $\tau_p$ turned out to be approximately twice as high (59.3 ns). The difference in these times is clearly seen in Fig. 1a: the pressure reaches the value $p_J$ appreciably later than the degree of conversion visually reaches unity. The reason for this difference is illustrated in Fig. 1b. As the phase points follow the Rayleigh line, which is tangential to the detonation adiabat to the Jouguet point, small deviations of pressure near this point $(p - p_J)$ have a lower order of smallness than the deviations of the degree of conversion, namely, $(p - p_J) \propto \sqrt{1-\lambda}$. In the case of exponential approaching of the Jouguet point, the characteristic time $\tau_p$ should be approximately $2\tau_\lambda$. It should be noted that the characteristic times of changing of the specific volume and particle velocity in the reaction zone coincide with $\tau_p$ because of the linear relationships of these quantities with pressure in the steady reaction zone.

Actually, we should not expect the time $T$ determined from the dependence $u(t)$ to coincide with the true reaction time $\tau$. The time $T$ is closer to $\tau_p$ (which is natural), but it differs from the latter because wave passage to an inert substance is an essentially unsteady and nonlinear gas-dynamic process. The considered example shows how important it is to indicate clearly the procedure determining the kinetic characteristics from experiments. Some definite results can be obtained only by means of direct fitting of kinetics reproducing the dependences $u(t)$ or the profiles $p(x)$ or $u(x)$ in the full gas-dynamic calculation of the process. Unfortunately, such a complete study is seldom performed, and many researchers obtain only rough estimates, for instance, indicating the time when the Jouguet state is reached (in the example considered here, 160 ns), which can be partially responsible for the large scattering of reported data.

Involvement of differential kinetics leads to drastic enhancement of the reaction in the wave front. Figure 2 shows the calculations for the kinetics variant with $b = 3$, where the degree of conversion in the front reaches 0.7. Indeed, in the profile of $\lambda$, we can see a jump of this size "smeared" over several cells. The chemical peak decreases noticeably.

In the phase diagram, the points mapping the wave front move upward to the place of intersection of the line $R$ with the partial reaction adiabat $S_p$ on which the degree of conversion is finite and corresponds to Eq. (5), rather than with the frozen adiabat $S$. The equation for $S_p$ has the form

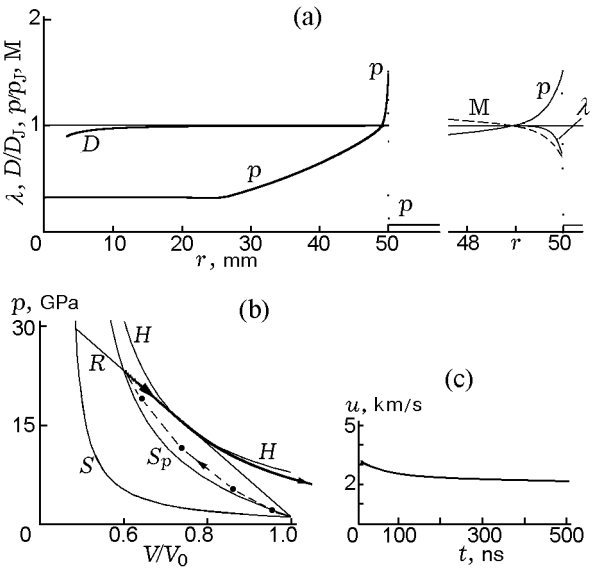


**Fig. 2.** Calculation variant with a reduced chemical peak. Nonclassical kinetics (4) with $b = 3$: (a) distributions of parameters; (b) phase diagram; (c) record of interface velocity.

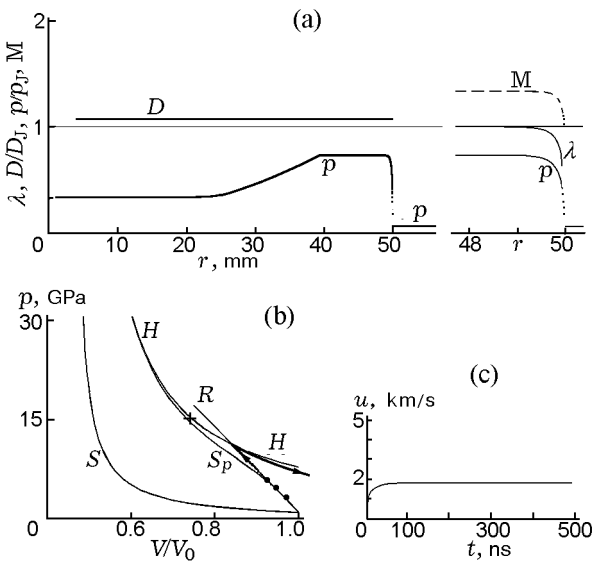


**Fig. 3.** Results of calculations of weak detonation. Nonclassical kinetics (4) with $b = 11$: (a) distributions of parameters; (b) phase diagram; (c) record of interface velocity.

$$p = [2(\gamma-1)Q(1-\exp(-b(1-V/V_0))) + p_0((\gamma+1)V_0-(\gamma-1)V)] /[(\gamma+1)V-(\gamma-1)V_0]. \quad (8)$$

The initial slope of $S_p$ is greater than the slope of $S$ owing to the difference between the thermodynamic frozen velocity of sound $c = \sqrt{\gamma pV}$ and the velocity of propagation of disturbances $c_E$ obtained if the differential mechanisms of reaction (6) are taken into account. In the vicinity of the initial point, the phase trajectory is tangent to the line $S_p$. A comparison of Figs. 1 and 2 shows that a partial reaction in the wave front leads to a less expressed chemical peak, but the Chapman–Jouguet state is reached, as well as the thermodynamic detonation velocity.

The characteristic reaction time based on the smooth portion of the profile $\lambda(x)$ is estimated as $\tau_\lambda = 33.6$ ns. The time $\tau_p = 68.4$ ns, as in the variant with $b = 0$, turns out to be approximately twice greater. For the dependence $u(t)$ (Fig. 2c), the characteristic time is $T = 83.2$ ns. The greater values of these times (as compared with the previous variant) are caused by certain deceleration of the reaction outside the wave front region. After initial compression in the wave front, the material expands in the reaction zone, and the differential term in the right side of Eq. (4) reduces the rate of conversion. As it follows from Fig. 2b, the specific volume in the smooth region of the reaction zone increases approximately by $\Delta V = 0.14$ cm$^3$/g. Assuming that the volume changes within the characteristic time $\tau_p$, we can use Eq. (4) to estimate the influence of the expansion effect on the kinetics as

$$\frac{1}{\tau_\lambda} = \frac{1}{\tau}\left(1 - b\frac{\Delta V}{V_0}\frac{\tau}{\tau_p}\right),$$

and the increase in $\tau_\lambda$ at $\tau_p = 68.4$ ns and $b = 3$ is approximately 23%, as compared with the variant with $b = 0$, which is consistent in the order of magnitude to the increase predicted by calculations.

As the contribution of the differential term to kinetics (4) increases, the partial conversion adiabat $S_p$ approaches the equilibrium adiabat $H$, which is inevitably accompanied by an increase in the initial slope of $S_p$. It is easy to demonstrate that the slope of $S_p$ becomes equal to the slope of the tangential line to $H$ drawn from the initial point at

$$b_* = (\gamma+1)\left(1 + \sqrt{1 + \frac{2\gamma p_0 V_0}{(\gamma^2-1)Q}}\right) = 7.778.$$

One can expect that the situation becomes qualitatively different at greater values of $b$. Namely, at $b > b_*$, the velocity of small perturbations $c_E$ exceeds the ideal detonation velocity $D_J$. The Chapman–Jouguet wave becomes unstable because the disturbances from the reaction zone can now overtake this wave. Now these disturbances form the wave front.

Figure 3 shows the results for the variant with $b = 11$, i.e., with a large contribution of differential kinetics. The wave rather rapidly transforms to the weak

detonation regime with the front velocity of 8.035 km/s (exceeding the Chapman–Jouguet velocity by 579 m/s). A gradual increase in pressure is observed instead of the chemical peak on the wave front after the initial drastic increase. The increasing segment is followed by a "plateau," and the maximum pressure is lower than that in the Chapman–Jouguet regime.

The phase points on the diagram in Fig. 3b from the initial state move upward along the ray $R$, which is practically tangent to the partial conversion adiabat $S_p$ at the point $(p_0, V_0)$. As the slope of $S_p$ is noticeably greater than the slope of the straight line tangential to the Hugoniot adiabat $H$ at the Jouguet point (denoted by the cross), the Chapman–Jouguet state cannot be reached. Instead, the phase trajectory reaches $H$ on its weak branch and then goes downward along the Poisson adiabat after the interval of constant parameters. The record of the interface velocity displays a smooth growth after the initial drastic increase, followed by a constant-velocity segment. The density of points gradually increases, and clear identification of the jump on the front is problematic.

Thus, Fig. 3 demonstrates the main classical features of the weak detonation regime [27]. It should be also noted that such regimes were not considered in [20] because the shock wave front thickness was neglected in that work. To obtain weak detonation, one needs full consideration of wave evolution from the initial perturbation with resolving the compression front structure.

The characteristic time $\tau_\lambda$ for this variant is 18.2 ns, the time $\tau_p$ is 22.1 ns, and the time of rise of the dependence $u(t)$ is 15.6 ns. All these times are noticeably smaller than $\tau$. This deviation is a result of a positive contribution of the differential term in kinetics (4) in the region of a smooth increase in density behind the front. An estimate similar to that performed above provides a decrease in $\tau_\lambda$ approximately to $0.44\tau$, which agrees with the calculation in terms of the order of magnitude. In this variant, the rule $\tau_p \approx 2\tau_\lambda$ is invalid because the line $R$ is no longer tangential to $H$.

As the weak detonation regime can be realized in principle owing to dissipation [15], it is of interest to clarify the comparative role of the compression factor and viscosity factor in our problem. For this purpose, we performed calculations with viscosity coefficient values $A = 8$–$128$, which corresponds to the shock wave width from 4 to 16 cells or (with the cell size used here) from 25 to 100 $\mu$m. The dependence of the velocity of the steady regime on viscosity was found to be rather weak: from 0.913 to 1.038 of the theoretical "inviscid" velocity $D_i = 8.803$ km/s corresponding to the contact point of the lines $R$ and $S_p$ at $b = 11$ ($D_i = c_E$ at the start of the reaction). An apparent reason for this difference is the influence of both viscosity and ignition conditions. In the calculations, we permanently tracked the $p$–$V$ diagram of the process, and the first phase point on the wave front from time to time was found to be on the standard adiabat $S$ rather than on the line $R$ or $S_p$, if the pressure at this point did not reach $p_i$. Certainly, the approximation of the ideal regime [20] is violated in these cases, and some reduction of the mean wave velocity should be expected. An increase in $p_i$ up to 1.1 decreases the wave velocity approximately by 4.3%, and a decrease in $p_i$ to 1.01 increases the wave velocity approximately by the same value. A higher value of $D_i$ at high viscosity can be associated with the direct effect of dissipation, as in [15], because the theoretical width of the compression front at $A = 128$ becomes comparable with the characteristic width of the reaction zone in a smooth flow ($D\tau_\lambda \approx 200$ $\mu$m). If we bear in mind these reservations, the above-given results for $A = 8$ are in reasonable agreement with the inviscid limit. The weak regime is mainly generated by a change in the dynamic properties of the medium owing to involvement of the volume rate of compression rather than by dissipation. Viscosity in this work just smears the shocks in which it is determined on what part of the detonation adiabat the reacting particle arrives

Let us pay special attention to the existence of the sonic point in the weak detonation wave. The wave can be presented as a sequence of small perturbations, where the first perturbation has a velocity $D_i$ with respect to the material at rest, and the subsequent perturbations move with the current velocities $c_E$ with respect to the material, which is already set into motion. In an ideal formulation, as $p_i \to 1$, the starting value of M in the reaction zone should be equal to unity by virtue of the equality $D_i = c_E(p_0, V_0, \lambda = 1)$. In the course of the reaction, the Mach number M increases, as is seen from Fig. 3a. Therefore, except for one point, the entire flow behind the front is supersonic (M > 1). Before the reaction starts, the velocity of sound ahead of the front is low ($c = \sqrt{\gamma p_0 V_0} = 1.643$ km/s should be used here rather than $c_E$), and also M > 1 ahead of the wave. Therefore, in an ideal situation, we have a jump to the line M = 1 from above and reflection from this line to the domain with M > 1 instead of a transition through the sonic point. In this aspect, the situation differs from the classical case considered in [27] where the wave velocity was dictated by an external source of initiation, and the entire flow was rigorously supersonic. In the real calculation illustrated in Fig. 3, the wave velocity is slightly smaller than $D_i$, which was already discussed above. Because of discretization, however, the first calculated value behind the front is slightly greater than unity; thus, the Mach number contour in Fig. 3 provides

a qualitatively correct description of the wave structure.

A transition to weak detonation regimes in calculation occurred at $b = 8.75$, which is slightly greater than the theoretical value equal to 7.778. This minor difference is also related to the loss of approximation because of large gradients in the wave front.

## 4. DISCUSSION

The behavior of the model is completely consistent with the interpretation of the experimental results [5–14] proposed by the authors of these papers, with the only difference that different regimes are obtained owing to the use of nonclassical kinetics. The qualitative agreement of the calculated and experimental results can be considered as an additional justification of the analysis performed by the experimenters. It should be noted that transitions between different regimes within the single model are provided by changing the only governing parameter $b$.

The alternative explanation [28] is based on the assumption of intersection of the shock and detonation adiabats if the initial HE density is sufficiently high. Without going into details of the concept developed by Kuz'mitskii [28], we can state that he considered only one intersection, whereas cases observed later, where a nonclassical profile is observed within a certain interval of initial densities, require double intersection of the adiabats. For such situations, the explanation proposed in [28] seems to be artificial. According to later data [10–13], the main factor for nonclassical regimes is the structure of the explosive, whereas the pressing density has an indirect effect because it affects the structure. Profiles with increasing pressure were obtained under various conditions, including rather low densities. Therefore, the main factor leading to the emergence of nonclassical regimes has a kinetic nature rather than a thermodynamic nature declared in [28].

Good agreement of the predicted records of interface velocity (obtained for a very simple and rather rough formulation) and the data obtained in [5–14] should be noted. It can be expected that involvement of differential kinetics would provide quantitative agreement as well if real gas properties were taken into account. Thus, it is possible to determine macrokinetics on the basis of VISAR experimental data with allowance for the final reaction in the front, including clearly nonclassical weak detonation regimes. It should be borne in mind that rough visual estimates of the reaction time based on interface velocity records can differ from the real value noticeably. As shown above, such deviations are usual even if the changes in the parameters in the reaction zone do not directly affect the course of the reaction. Therefore, the kinetics should be extracted by comparing experimental and calculated curves.

In weak regimes, the velocity of wave propagation is no longer fixed by thermodynamic conditions, instead, it depends on the kinetics. As was noted in [27], high-velocity weak detonation waves could propagate in principle owing to the fast transport of electrons or photons. This possibility is prevented by a practical fact: a very small fraction of energy is transferred under typical conditions of "chemical" detonation to these fast exciting agents. If the energy is increased, however, radiative transport can become the main mechanism [29].

Similarly, in the case of detonation in a porous medium, a natural candidate for the role of a fast transporting agent is mesoscopic flows. The wave front in a porous structure is a complex non-one-dimensional system in which the reaction can propagate not owing to heating induced by compression, but also owing to inhomogeneities, such as microjets overtaking the main front. Advanced propagation of microjets raises no doubts (see, e.g., [30]). As it follows from experience, their effectiveness for front propagation is insufficient in most cases (which allows us to speak about "normal" detonation). Nevertheless, the experiments [5–14] show that weak regimes can be obtained by satisfying certain special conditions, such as sufficient sensitivity of the HE to such propagation agents, concentration of potentially active spots, certain particle size, and certain structure of the pore space. Apparently, weak detonation waves were not observed in all HEs (the best example is TNETB) because a combination of several conditions had to be satisfied; moreover, they were observed in rather narrow ranges of parameters. It should be noted that weak regimes in our calculations were obtained at sufficiently large values of the dimensionless governing parameter ($b \approx 10$); therefore, they constitute somewhat exotic cases. Vice versa, regimes with the Chapman–Jouguet velocity, but with a reduced chemical peak are fairly typical.

In the above-described model, the "smeared" wave front in the calculations should be understood as a rough averaged presentation of a real non-one-dimensional front, which takes into account microjets as well. Though the condition of involvement of the reaction was formally identical in all calculations, but the state in the wave at large values of $b$ (i.e., with a significant contribution of the reaction in the front) evolves in a different manner because the velocity of propagation of disturbances in the reacting medium becomes greater than the thermodynamic velocity of the wave $D_{\text{J}}$. We can say that a substance with a sufficiently high sensitivity to microjets is modeled in this way.

The jets can be expected to play the minimum role in HEs with the greatest density, in particular, in agatized HEs. In [1, 2], the chemical peak was not registered in dense HEs, which may be a consequence of a rather fast reaction within the limits of experimental resolution. Fedorov [4], however, reported a normal chemical peak in agatized HMX. A clear increase in the parameters of agatized RDX and HMX was observed in [3]. Thus, the experimental information on this topic is contradictory, and the issue requires further investigations.

This work was supported by the Russian Foundation for Basic Research (Grant No. 12-03-00077) and by the Research Program No. 2 of the Presidium of the Russian Academy of Sciences (Grant No. 7).

## REFERENCES

1. B. G. Loboiko and S. N. Lubyatinsky, "Reaction Zones of Detonating Solid Explosives," Fiz. Goreniya Vzryva **36** (6), 45–64 (2000) [Combust., Expl., Shock Waves **36** (6), 716–733 (2000)].
2. C. M. Tarver, R. D. Breithaupt, and J. W. Kury, "Detonation Waves in Pentaerythritol Tetranitrate," J. Appl. Phys. **81** (11), 7193–7202 (1997).
3. V. K. Ashaev, G. S. Doronin, and A. D. Levin, "Detonation Front Structure in Condensed High Explosives," Fiz. Goreniya Vzryva **24** (1), 95–99 (1988) [Combust., Expl., Shock Waves **24** (1), 88–91 (1988)].
4. A. V. Fedorov, "Detonation Wave Structure in Liquid Homogeneous, Solid Heterogeneous and Agatized HE," in *Proc. of 12th Int. Detonation Symp., San Diego, CA, 2005*, pp. 230–233.
5. A. V. Utkin, "Effect of Initial Density on the Structure of Detonation Waves in Heterogeneous HEs," in *Chemical Physics of Combustion and Explosion, Proc. 12th Symp. on Combustion and Explosion*, Chernogolovka (2000), Part II, pp. 168–170.
6. A. V. Utkin, S. V. Pershin, and V. E. Fortov, "Change in the Structure of the Detonation Wave in 2′,2′,2′-trinitroethyl-4,4,4-trinitrobutyrate with increasing initial density," Dokl. Akad. Nauk **374** (4), 486–488 (2000).
7. A. V. Utkin, S. A. Kolesnikov, and V. E. Fortov, "Structure of a Steady Detonation Wave in Pressed RDX," Dokl. Akad. Nauk **381** (6), 760–762 (2001).
8. A. V. Utkin, S. A. Kolesnikov, S. V. Pershin, and V. E. Fortov, "Influence of Initial Density on the Reaction Zone for Steady-State Detonation of High Explosives," in *Proc. of 12th Int. Detonation Symp., San Diego, CA, 2002*, pp. 175–182.
9. A. V. Utkin, S. A. Kolesnikov, and S. V. Pershin, "Effect of the Initial Density on the Structure of Detonation Waves in Heterogeneous Explosives," Fiz. Goreniya Vzryva **38** (5), 111–118 (2002) [Combust., Expl., Shock Waves **38** (5), 590–597 (2002)].
10. S. A. Kolesnikov, A. V. Utkin, A. V. Anan'in, S. V. Pershin, and V. E. Fortov, "Reaction Zone of Steady-State Detonation Waves in Dinitrodiazapentane and RDX," in *Proc. Shock Compression of Condensed Matter, Portland, OR, 2003*; AIP Conf. Proc., Vol. 706 (2003), pp. 851–854.
11. A. V. Utkin, A. V. Anan'in, S. A. Kolesnikov, and S. V. Pershin, "Structure of Detonation Waves in Individual and Composite Pressed HEs," in *Extreme States of Matter. Detonation. Shock Waves, Proc. VII Khariton's Topical Scientific Readings* (Sarov, 2005), pp. 10–14.
12. S. A. Kolesnikov, A. V. Utkin, and A. V. Ananin, "Non-Classical Steady-State Detonation Regimes in TNETB," in *Proc. of 13th Int. Detonation Symp., Norfolk, VA, 2006*, ONR 351-07-01, pp. 422–426.
13. A. V. Utkin, V. M. Mochalova, and A. V. Ananin, "Reaction Zone Structure for Pressed HE and Mixtures of High Explosives with Additions," in *Proc. of 13th Int. Detonation Symp., Norfolk, VA, 2006*, ONR 351-07-01, pp. 415–421.
14. V. M. Mochalova, A. V. Utkin, and A. V. Anan'in, "Effect of the Degree of Dispersion on the Detonation Wave Structure in Pressed TNETB," Fiz. Goreniya Vzryva **43** (5), 90–95 (2007) [Combust., Expl., Shock Waves **43** (5), 575–579 (2007)].
15. F. A. Williams, *Combustion Theory* (Westview Press, 1985).
16. E. L. Lee and C. M. Tarver, "Phenomenological Model of Shock Initiation in Heterogeneous Explosives," Phys. Fluids **23**, 2362–2371 (1980).
17. V. Yu. Klimenko, "Multiprocess Model of Detonation (Version 3)," in: *Shock Compression of Condensed Matter-1995*, Ed. by S. C. Schmidt, W. C. Tao, AIP Conf. Proc., Vol. 370, Part 2, pp. 361–364.
18. V. G. Morozov, I. I. Karpenko, et al., "Theoretical Justification of the Phenomenological Model of Shock Wave Sensitivity of a TATB-Based Heterogeneous HE with Allowance for Single and Double Shock-Wave Loading, Including Intermediate Unloading," Khim. Fiz. **14** (2–3), 32–39 (1995).
19. A. P. Ershov and D. A. Medvedev, "On Kinetics of Chemical Reactions During Detonation," Pis'ma Zh. Tekh. Fiz. **35** (3), 60–66 (2009).
20. A. P. Ershov, "Macrokinetics of Fast Reactions," Fiz. Goreniya Vzryva **46** (6), 49–59 (2010) [Combust., Expl., Shock Waves **46** (6), 656–665 (2010)].
21. V. S. Trofimov, "Possibility of Reaction Acceleration and Diffusion in the Shock Front of Detonation,"

in *Detonation. Critical Phenomena. Physicochemical Transformations in Shock Waves* (Chernogolovka, 1978), pp. 11–16.
22. V. S. Trofimov and G. P. Trofimova, "Possibility of Decomposition of Cast TNT in a Shock," Fiz. Goreniya Vzryva **16** (2), 92–99 (1980) [Combust., Expl., Shock Waves **16** (2), 215–221 (1980)].
23. A. V. Vorob'ev, V. S. Trofimov, K. M. Mikhailyuk, et al., "Investigation of Detonation Initiation in Cast Trotyl by a Dynamic Method. 1. Formulation of the Problem and Experimental Procedure," Fiz. Goreniya Vzryva **21** (2), 106–116 (1985) [Combust., Expl., Shock Waves **21** (2), 227–235 (1985)].
24. R. Richtmyer and K. Morton, *Difference Methods for Initial Value Problems* (Springer, New York, 1967).
25. L. D. Landau and E. M. Lifshits, *Course of Theoretical Physics*, Vol. 6: *Fluid Mechanics* (Pergamon Press, Oxford-Elmsford, New York, 1987).
26. Ya. B. Zel'dovich and Yu. P. Raizer, *Physics of Shock Waves and High-Temperature Hydrodynamic Phenomena* (GIFML, Moscow, 1955; Academic Press, New York, 1967).
27. Ya. B. Zel'dovich and A. S. Kompaneets, *Theory of Detonation* (Gostekhizdat, Moscow, 1955; Academic Press, New York, 1960).
28. I. V. Kuz'mitskii, "Dependence of the Time-Space Structure of the Chemical-Reaction Zone on the Initial Density of the Explosive," Fiz. Goreniya Vzryva **40** (4), 106–111 (2004) [Combust., Expl., Shock Waves **40** (4), 467–472 (2004)].
29. L. P. Feoktistov, "Thermonuclear Detonation," Usp. Fiz. Nauk **168** (11), 1247–1255 (1998).
30. A. V. Fedorov, "Parameters of the von Neumann Peak and Detonation Wave Front Structure in Condensed High Explosives," Khim. Fiz. **24** (10), 13–21 (2005).